# An Assessment of Uncertainty for a Head End Process in the Pyroprocessing

Wonjong Song, Hoyoung Shin, Myeonghyeon Woo, Moosung Jae[*]
*Department of Nuclear Engineering, Hanyang University, Seoul, 04763, Korea*
[*]*Corresponding author: jae@hanyang.ac.kr*

## 1. Introduction

After 2019, spent fuel pools of nuclear power plants in Korea will gradually be full of spent fuels. So, Korea has been developing the pyroprocessing that changes spent fuels of a LWR to fuels of a SFR. In the pyroprocessing, nuclear material accountancy considering uncertainty is important because this is controlled by weight unit. Accordingly, a method using a (Pu/$^{244}$Cm) mass ratio has been studied to detect Pu mass indirectly. But, the heterogeneous (Pu/$^{244}$Cm) mass ratio of fuel rods appears by height and enrichment when fuel rods are burned [1].

In this study, we analyzed the heterogeneity by height of fuel rods according to burnup and cooling periods based on computer simulation codes and calculated the uncertainty of nuclear material accountancy in a head end process of the pyroprocessing by random sampling simulations.

## 2. Methods and Results

### 2.1 Computer simulation codes

The MCNP and the CINDER'90 were used to simulate a fuel burnup process of a LWR [2,3]. The MCNP based on Monte Carlo method is a particle transport analysis code that generates random numbers to describe behavior of particles and estimate a solution of the Boltzmann transport equation. The CINDER'90 performs a reactor irradiation calculation and solves the Bateman equation to track nuclide change in materials. In this study, the MCNP was selected as the analysis code of neutron transport calculation, and the CINDER'90 was selected as the analysis code of nuclide change in materials for the fuel assembly burnup process.

A link system was used to simulate the fuel assembly burnup process between the MCNP and the CINDER'90. The MCNP calculates neutron flux, reaction rate, and Q-value at each time step. Using this information, the CINDER'90 calculates the amount of nuclide inventory at each time step and gives results of nuclide change in materials to the MCNP as input file to perform neutron transport calculation. This link system assumes that the neutron flux is constant at each time step. However, generation of $^{135}$Xe has a great influence on the neutron flux and criticality. Therefore, when obtaining the neutron flux at each time step, Predictor-Corrector method was used which calculates a ratio of nuclide at the midpoint of each time step. A scheme of the link system between the MCNP and the CINDER'90 is showed in Fig. 1.
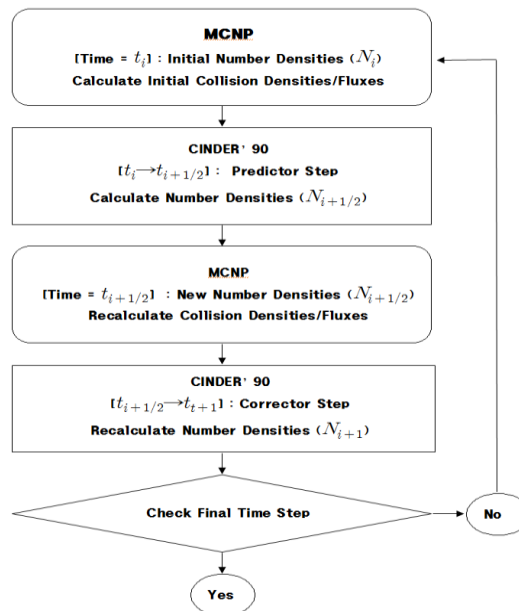


Fig. 1. Scheme of the link system between the MCNP and the CINDER'90

Intervals of each time step are controlled by the TIME input variable among the BURN CARD options of the MCNP. Because $^{135}$Xe has a very high neutron absorption cross section, the time interval at beginning of cycle is defined shortly to satisfy equilibrium state of $^{135}$Xe concentration [4].

### 2.2 Reference reactor

Hanbit unit 3 whose reactor type is OPR1000 was selected as a reference reactor. By analyzing the nuclear design report of Hanbit unit 3, we found reactor characteristic factors as well as A0, B0, and C0 fuel assembly characteristic factors. Table Ⅰ and Ⅱ show the researching results [5].

Table Ⅰ. OPR1000 characteristic factors

| Characteristic factor | Value |
|---|---|
| Thermal Power [MW$_{th}$] | 2815 |
| Inlet/Outlet Temperature [℃] | 295.8/327.3 |
| Pellet/Clad Material | UO$_2$/ZIRLO |
| Pellet Density [g/cm$^3$] | 10.44 |
| Pellet Diameter [cm] | 0.826 |
| Clad Inner/Outer Diameter [cm] | 0.843/0.970 |
| Active Length [cm] | 381 |
| Fuel Pitch [cm] | 1.285 |
| Assembly Array | 16x16 |

Table Ⅱ. Fuel assembly information

| Assembly type | Enrichment [w% $^{235}$U] | Burnup [MWd/kgU] | Number of Fuel Rods |
|---|---|---|---|
| A0 | 1.42 | 11.6~14.2 | 236 |
| B0 | 2.92/2.42 | 37.1~39.7 | 184/52 |
| C0 | 3.43/2.93 | 33.8~44.1 | 184/52 |

Table Ⅲ. Axial mesh size of fuel assembly

| Burnup Region | Mesh Size [cm] | Cumulative Height [cm] | Temperature [℃] | Density [g/cm$^3$] |
|---|---|---|---|---|
| 1~5 | 1 | 5 | 295.8 | 735.0~734.9 |
| 6~10 | 5 | 30 | 295.8~296.2 | 734.9~734.2 |
| 11~13 | 10 | 60 | 296.4~297.3 | 733.7~731.8 |
| 14~15 | 15 | 90 | 298.1~299.3 | 730.2~727.9 |
| 16~17 | 20 | 130 | 300.8~302.9 | 724.7~720.4 |
| 18~21 | 30.25 | 251 | 305.8~317.2 | 714.1~687.1 |
| 22~23 | 20 | 291 | 320.1~322.2 | 679.7~674.2 |
| 24~25 | 15 | 321 | 323.7~324.9 | 669.9~666.7 |
| 26~28 | 10 | 351 | 325.7~326.6 | 664.4~661.7 |
| 29~33 | 5 | 376 | 326.8~327.2 | 660.9~659.8 |
| 34~38 | 1 | 381 | 327.2 | 659.8~659.7 |

*2.3 Input file for computer codes*

The burn process was simulated by a fuel assembly unit as in Fig. 2. Because computing time of the burnup process simulation for a full core is very long. Also, radial symmetry and infinite arrangement of the fuel assemblies were assumed in the burnup calculations because the fuel assemblies would be burned uniformly in the core. Therefore, thermal power of 16MW was assumed for each fuel assembly.

To find out the heterogeneity by height of the fuel assembly, middle burnup regions were divided into long lengths, and end burnup regions were divided into short lengths. Because the neutron flux at the end burnup regions is steeper than the middle burnup regions. As a result of division, the total number of burnup regions is 38 as in Table Ⅲ.

As the temperature of coolant increases with the upper part of the core, the cross section and density of coolant change. These changes affect the neutron flux. Therefore, average temperatures of each burnup region were calculated by equation 1 using boundary conditions such as inlet and outlet temperature. This is because the MCNP can't set continuous temperature profile. The density of coolant corresponding to the temperature is found at the NIST database.

$$T(z) = T_{inlet} + Const \times \left[ cos \left( \frac{\pi z}{H_{active}} \right) + 1 \right] \quad (1)$$

In this study, the burnup periods were set to 400, 500, 600, 700, and 800 days, and the cooling periods were set to 0, 10, 20 ,30, and 40 years, respectively.
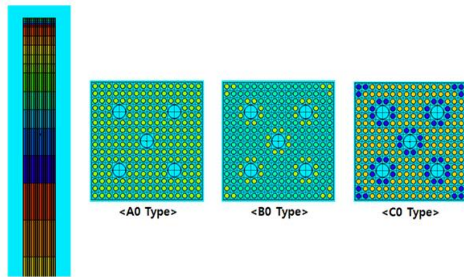


Fig. 2. The MCNP input file modeling for each fuel assembly

*2.4 Heterogeneous results by height of fuel rods*

As a result of the burnup process, the heterogeneity by height appeared for all fuel assemblies. Fig. 3 is a result of the heterogeneous (Pu/$^{244}$Cm) mass ratio of all fuel assemblies for 600 days of burnup and 20 years of cooling. The lower the concentration, the smaller the average (Pu/$^{244}$Cm) mass ratio and the greater the (Pu/$^{244}$Cm) mass ratio difference.
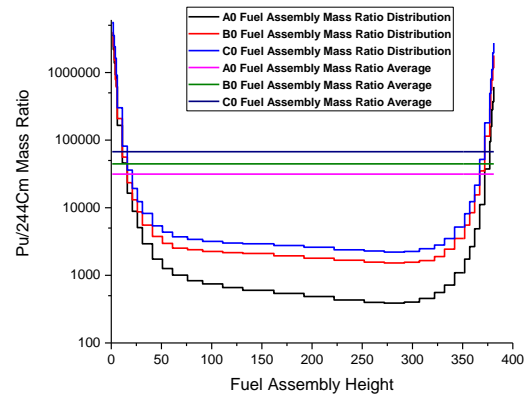


Fig. 3. (Pu/244Cm) mass ratio results of each fuel assembly

The shorter the burnup periods and the longer the cooling periods, the greater the (Pu/$^{244}$Cm) mass ratio difference.

Table Ⅳ. Mass ratio difference results of each fuel assembly

| FA | Cooling Periods | Burnup Periods | | | | |
|---|---|---|---|---|---|---|
| | | 400 | 500 | 600 | 700 | 800 |
| A0 | 0 | 6.4x10$^4$ | 2.1x10$^4$ | 8.6 x10$^3$ | 4.9 x10$^3$ | 2.9 x10$^3$ |
| | 10 | 6.7 x10$^4$ | 2.1 x10$^4$ | 8.9 x10$^3$ | 5.1 x10$^3$ | 3.0 x10$^3$ |
| | 20 | 6.9 x10$^4$ | 2.2 x10$^4$ | 9.2 x10$^3$ | 5.2 x10$^3$ | 3.1 x10$^3$ |
| | 30 | 7.0 x10$^4$ | 2.3 x10$^4$ | 9.4 x10$^3$ | 5.3 x10$^3$ | 3.1 x10$^3$ |
| | 40 | 7.1 x10$^4$ | 2.3 x10$^4$ | 9.5 x10$^3$ | 5.4 x10$^3$ | 3.2 x10$^3$ |
| B0 | 0 | 9.3 x10$^3$ | 3.9 x10$^3$ | 2.4 x10$^3$ | 1.2 x10$^3$ | 8.8 x10$^2$ |
| | 10 | 9.6 x10$^3$ | 4.0 x10$^3$ | 2.5 x10$^3$ | 1.3 x10$^3$ | 9.1 x10$^2$ |
| | 20 | 9.8 x10$^3$ | 4.1 x10$^3$ | 2.6 x10$^3$ | 1.3 x10$^3$ | 9.4 x10$^2$ |
| | 30 | 1.0 x10$^4$ | 4.2 x10$^3$ | 2.6 x10$^3$ | 1.3 x10$^3$ | 9.5 x10$^2$ |
| | 40 | 1.0 x10$^4$ | 4.2 x10$^3$ | 2.7 x10$^3$ | 1.3 x10$^3$ | 9.6 x10$^2$ |
| C0 | 0 | 7.3 x10$^3$ | 3.8 x10$^3$ | 2.6 x10$^3$ | 1.3 x10$^3$ | 1.0 x10$^3$ |
| | 10 | 7.5 x10$^3$ | 4.0 x10$^3$ | 2.7 x10$^3$ | 1.3 x10$^3$ | 1.1 x10$^3$ |
| | 20 | 7.6 x10$^3$ | 4.1 x10$^3$ | 2.7 x10$^3$ | 1.4 x10$^3$ | 1.1 x10$^3$ |
| | 30 | 7.7 x10$^3$ | 4.1 x10$^3$ | 2.8 x10$^3$ | 1.4 x10$^3$ | 1.1 x10$^3$ |
| | 40 | 7.8 x10$^3$ | 4.2 x10$^3$ | 2.8 x10$^3$ | 1.4 x10$^3$ | 1.1 x10$^3$ |

*2.5 Head end process simulation and uncertainty result*

The head end process of the pyroprocessing is composed of chopping step, voloxidation step, and homogenization step [6]. Among these steps, the chopping step was assumed to operate by 50kgHM/batch [7]. The entire head end process is firstly the chopping step where one fuel assembly is decomposed into 1cm long $UO_2$ pellets, resulting in a total of 89,916 $UO_2$ pellets. Secondly, in the voloxidation step, 9,144 $UO_2$ pellets corresponding to 50kgHM are randomly selected and oxidized to $U_3O_8$ powder. Finally, in the homogenization step, the $U_3O_8$ powder is mixed homogeneously. And, we conducted simulations of the voloxidation step. In these simulations, 9,144 pellets were randomly sampled for each fuel assembly 1,000 times, and the uncertainties of the Pu mass, the $^{244}$Cm mass, and the (Pu/$^{244}$Cm) mass ratio were calculated. Table Ⅴ and Fig. 4~9 are results of random samplings of all fuel assemblies. For the results fitting, we used normal distribution, respectively.

Table Ⅴ. Results of random sampling for voloxidation step

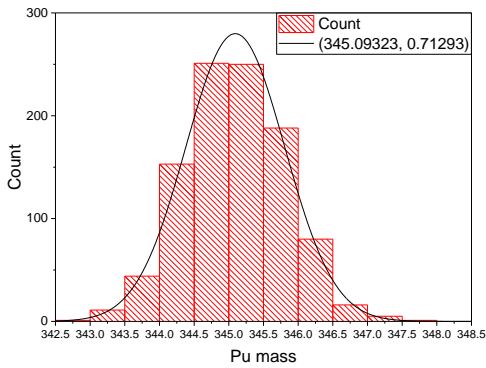| Fuel Assembly | Pu | | $^{244}$Cm | | Ratio |
|---|---|---|---|---|---|
| | Mean [g] | SD [%] | Mean [g] | SD [%] | SD [%] |
| A0 | 345.09 | 0.2066 | 0.56 | 0.5563 | 0.5935 |
| B0 | 321.07 | 0.1867 | 0.15 | 0.4796 | 0.5147 |
| C0 | 314.66 | 0.1915 | 0.10 | 0.4807 | 0.5174 |



Fig. 4. Result of random sampling of A0 fuel assembly (Pu)
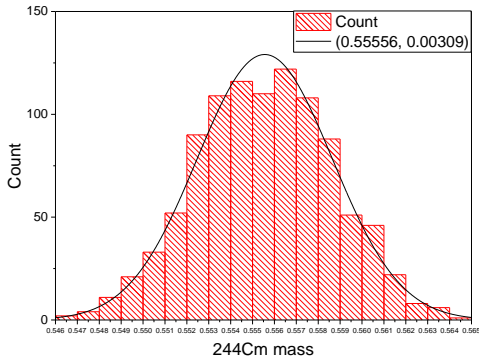


Fig. 5. Result of random sampling of A0 fuel assembly ($^{244}$Cm)
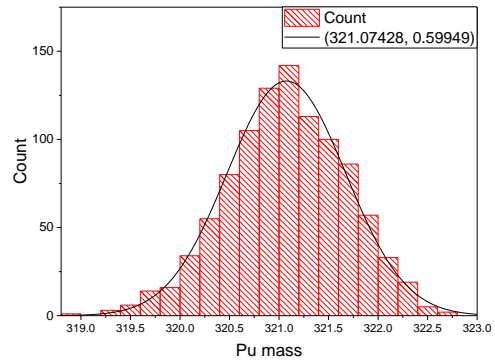


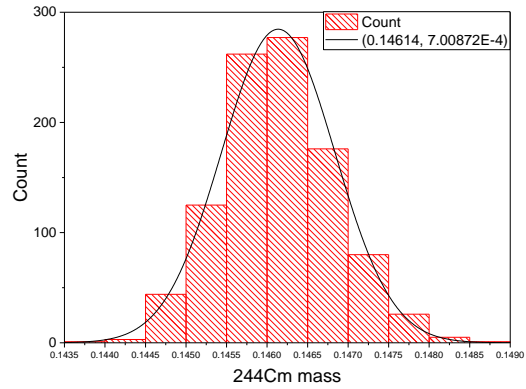Fig. 6. Result of random sampling of B0 fuel assembly (Pu)



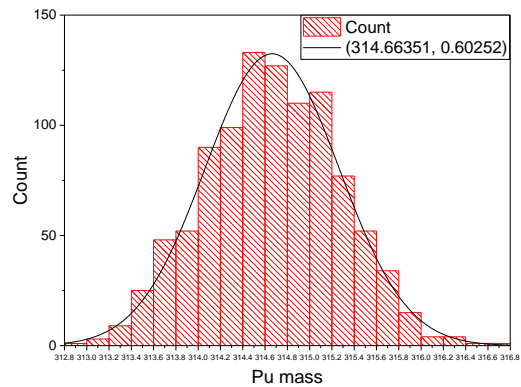Fig. 7. Result of random sampling of B0 fuel assembly ($^{244}$Cm)



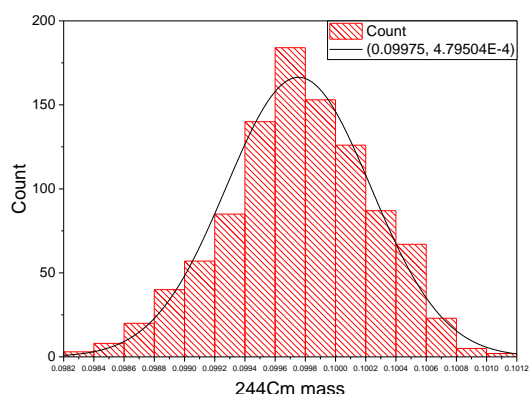Fig. 8. Result of random sampling of C0 fuel assembly (Pu)

Fig. 9. Result of random sampling of B0 fuel assembly ($^{244}$Cm)

We assumed that the $UO_2$ pellets which is at the same height or have same enrichment have an identical nuclide composition. Therefore, comparing the B0 and C0 fuel assembly containing two enrichment levels, the uncertainty of the C0 fuel assembly with higher enrichment level is slightly greater. Also, as shown in Table Ⅳ, the uncertainty of the A0 fuel assembly is the largest because the enrichment level of A0 assembly is the lowest.

### 3. Conclusions

In this study, we confirmed that heterogeneous (Pu/$^{244}$Cm) mass ratio appeared after the fuel rods were burned. Also, the uncertainties resulted from the heterogeneous (Pu/$^{244}$Cm) mass ratio of the fuel assemblies were calculated by simulating the voloxidation step of the pyroprocessing. However, the identical nuclide composition, radial symmetry, and infinite arrangement of the fuel assemblies was assumed. So, if we divide the burnup regions shortly according to height of the fuel assembly and consider radial asymmetry, more realistic results will be obtained. Conclusively, a methodology of this study could be used to enhance the reliability of the nuclear material accountancy.

### Acknowledgements

### REFERENCES

[1] S. M. Woo, M. Fratoni, and J. Ahn, Development of Numerical Recipes for High Resolution Depletion Simulations of a PWR Fuel Rod by SERPENT, Department of Nuclear Engineering University of California Berkeley, 2015.

[2] Mckinney, G., Durkee, J. S., Hendricks, J. S., James, M. R., & Pelowitz, MCNPX USERS MANUAL Version 2.7.0. LA-CP-11-00438, LANL, Los Alamos, 2011.

[3] Wilson, W. B., Cowell, S. T., England, T. R., Hayes, A. C., & Moller, P., A manual for CINDER'90 version 07.4 codes and data. Manual LA-UR, 07-8412, 2007.

[4] Woo, S. M., & Ahn, J., Model Development for Pu-Mass Accountancy of Pyrometallurgical Processing with the Pu/Cm-244 Ratio Method, In Actinide and Fission Product Partitioning and Transmutation. Thirteenth Information Exchange Meeting, Seoul, Republic of Korea (pp. 23-26), 2014.

[5] Liang Zhang, Evaluation of High Power Density Annular Fuel Application in the Korea OPR-1000 Reactor, Thesis of Master of Nuclear Engineering at MIT, 2009.

[6] S. M. Woo, J. H. Ahn, Uncertainty of the Pu to $^{244}$Cm Ratio in Spent Fuel, IHLRWM 2015, Charleston, 2015.

[7] KAERI, Development of a Safeguards Approach for a Pyroprocessing Plant by IAEA Member State Support Program, Korea Atomic Energy Research Institute, 2012.